The Astrophysical Journal Supplement Series, 240:7 (8pp), 2019 January https://doi.org/10.3847/1538-4365/aaf0a1
© 2019. The American Astronomical Society. All rights reserved.

VUV Spectral Irradiance Measurements in H_2/He/Ar Microwave Plasmas and Comparison with Solar Data

Et-touhami Es-sebbar[1,2], Yves Bénilan[1], Nicolas Fray[1], Hervé Cottin[1], Antoine Jolly[1], and Marie-Claire Gazeau[1]
[1] Laboratoire Interuniversitaire des Systèmes Atmosphériques, LISA, UMR 7583, CNRS, Université Paris Est Créteil and Université Paris Diderot, Institut Pierre Simon Laplace, 61 Avenue du Général De Gaulle, F-94010 Créteil Cedex, France; ettouhamiessebbar@gmail.com
[2] Paul Scherrer Institute, Laboratory for Thermal Processes and Combustion, PSI, CH–5232 Villigen, Switzerland; ettouhami.essebbar@psi.ch
Received 2018 July 17; revised 2018 October 30; accepted 2018 November 8; published 2019 January 4

Abstract

Microwave plasmas with H_2 and H_2/rare gas mixtures are convenient sources of VUV radiation for laboratory simulations of astrophysical media. We recently undertook an extensive study to characterize microwave plasmas in an H_2/He gas mixture in order to optimize a VUV solar simulator over the 115–170 nm spectral range. In this paper, we extend our investigation to the effect of the addition of Ar into H_2/He plasma on the VUV spectral irradiance. Our study combines various optical diagnostics such as a VUV spectrometer and optical emission spectroscopy. Quantitative measurements of the spectral irradiance and photons flux in different mixtures are accomplished using a combination of VUV spectrometry and chemical actinometry. Results show that the Ar addition into H_2/He plasma largely affects the predominant emissions of the hydrogen Lyα line (121.6 nm) and H_2 ($B^1\Sigma_u$–$X^1\Sigma_g$) band (150–170 nm). While a microwave plasma with 1.4% H_2/He is required to mimic the entire VUV solar spectrum in the 115–170 nm range, the combination with 1.28% H_2/35% Ar/He is the best alternative to obtain a quasi-monochromatic spectrum with emission dominated by the Lyα line. The maximum of the spectral irradiance is significantly higher in the ternary mixtures compared to the binary mixture of 1.4% H_2/He. Further Ar increase yielded lower spectral irradiance and absolute photon fluxes. Our measured spectral irradiances are compared to VUV solar data in the 115–170 nm range, emphasizing the use of microwave plasmas in astrophysical studies and laboratory simulations of planetary atmospheres.

Key words: astrochemistry – plasmas – Sun: UV radiation – techniques: spectroscopic

1. Introduction

Spectral irradiance and photon flux of vacuum ultraviolet sources are crucial parameters in all photochemistry processes, astrophysical studies, and laboratory simulations of planetary atmospheres (Baratta et al. 2002; Cottin et al. 2003; Romanzin et al. 2010; Chen et al. 2014; Cruz-Diaz et al. 2014; Shi et al. 2015). Hydrogen Lyα sources (Lyα at 121.6 nm $\sim$ 10.2 eV or the H I line) simulating the solar spectrum have been widely used in laboratory experiments. Low-temperature plasmas based on H_2 mixed with noble gases have been developed for a long time as a continuous Lyα source, where the corresponding intense line emission between the first excited and the ground state of the ($2p\,^2P_0$) $\rightarrow$ ($1s\,^2S$) transition can be produced by electrical discharges. Microwave, low-radio-frequency (rf), micro-hollow cathode, and dielectric barrier plasmas have been commonly used as convenient Lyα sources (Davis & Braun 1968; Bergonzo et al. 1992; Hollander & Wertheimer 1994; Fozza et al. 1998; El-Dakrouri et al. 2002; Yan et al. 2002; Rahman et al. 2004; McCarthy et al. 2005). Microwave plasmas are often preferred because they exhibit low gas temperatures and require only simple and non-expensive equipment. Nevertheless, one limitation of Lyα laboratory experiments is that the emission spectrum is not well-defined (Baratta et al. 2002; Cottin et al. 2003). Indeed, photons flux and spectral irradiance variations for different plasma conditions are important for understanding the photochemistry initiated by such irradiation. Particularly, fully incorporating knowledge of the wavelength dependence of the measured spectral data from the microwave plasma into astrophysical pursuits is important for VUV irradiation of ice analogs (Fayolle et al. 2011, 2013; Bertin et al. 2012). It has been shown that the large discrepancy in the photodesorption yields of CO ice, up to two orders of magnitude (Öberg et al. 2007, 2009; Muñoz Caro et al. 2010; Chen et al. 2014; Ligterink et al. 2015; Paardekooper et al. 2016), may result from their unresolved wavelength dependence (Fayolle et al. 2011; Ligterink et al. 2015). Consequently, the energy dependence of photodesorption rates is crucial for astrochemical models. A detailed quantification of the VUV irradiation source spectrum is required to determine quantitatively accurate photodesorption rates.

While most experimental studies on discharge lamps have dealt with the characterization of relative line intensities (Davis & Braun 1968; Hollander & Wertheimer 1994; El-Dakrouri et al. 2002), the spectral irradiance and photon flux have rarely been studied (Es-sebbar et al. 2015; Ligterink et al. 2015). In order to measure the absolute flux of photons, it is possible to use calibrated silicon photocathode detectors (Cottin et al. 2003) or chemical optical actinometry (Baratta et al. 2002; Cottin et al. 2003; Rajappan et al. 2010; Romanzin et al. 2010; Es-sebbar et al. 2015). The latter quantifies the production rate of the photodissociation species. Chemical actinometry is a non-invasive method, and requires only simple spectroscopic equipment. Carbon dioxide (CO_2), dioxygen (O_2), and nitrous oxide (N_2O), which are often used as gas actinometers, have well known photodissociation cross sections.

Earlier, we derived the photon flux at Lyα in the He/H_2 (98/2%) microwave plasma from FTIR spectroscopy using carbon dioxide as a gas actinometer (Romanzin et al. 2010). More recently, we determined the spectral irradiance along with photon flux in the microwave plasma of a He/H_2 (98/1%) mixture using the same actinometer (Es-sebbar et al. 2015). In the present experimental work, we examine a He/H_2

microwave discharge with the addition of Ar, aiming to measure spectral irradiances in ternary mixtures. The purpose of adding Ar into H_2 microwave plasmas is to help the impedance matching of the microwave power supply and stabilize the discharge; this can cause a change in fundamental parameters such as the gas density and temperature (Thomas et al. 1997; Fozza et al. 1998). The VUV emission spectra are first measured with a vacuum spectrometer for a wide range of experimental conditions. Then, we derive the spectral irradiance and photon flux using chemical actinometry based on CO_2 photodissociation by measuring the variation of the production rate of CO. Special attention is given to the optical emission spectroscopy (OES) of excited species, in particular the role of Ar metastables and their potential properties, to produce a powerful and quasi-monochromatic VUV source. In Section 2, we briefly describe the experimental setup; in Section 3 we present our results and compare them to the actual solar emission spectrum; and in Section 4 we provide our conclusions.

2. Experimental

The experimental setup has been described in a previous publication (see Es-sebbar et al. 2015), so only details relevant to the present experiment are given here. It consists of a microwave plasma source, a VUV spectrometer in the 115–200 nm range, an OES setup in the visible-near-infrared domain over 300–900 nm (see Figures 1(a)–(b)), and finally a FTIR spectrometer for actinometry to measure the spectral irradiance (see Figure 1(c)). The plasma is obtained in a quartz tube (internal diameter $\phi_{in} = 8$ mm, external diameter $\phi_{ext} = 10$ mm and length = 20 cm) in which the flow of H_2/He/Ar gases is injected (maximum impurities: $O_2 < 2$ ppm, $H_2O < 3$ ppm and $CH_4 < 0.5$ ppm; Alphagaz^{TM} 1). The gas flow rates, varying from 0.2 to 40 sscm (standard $cm^3\ min^{-1}$), are controlled by mass flow controllers (MKS 1179B). The gas pressure is measured using a Baratron (MKS 722A).

The microwave excitation is coupled to the quartz tube through a McCarrol-Cavity device (Opthos Instruments, Inc.) that is operated with a microwave generator at 2.45 GHz. Its maximum output power is 300 W. The discharge tube is cooled by an air flow to avoid any change in wall temperature. The light from the plasma is analyzed either by a VUV monochromator (Horiba-Jobin-Yvon, H20-UVL) separated from the microwave plasma by a MgF_2 window (cutoff near 115 nm) or by an optical fiber focused by means of two lenses on a 20 μm entrance slit of a JY-HR-1000 spectrometer (1 m focal length). The latter is equipped with a 1800 groves/mm grating and a Hamamatsu photomultiplier tube (R936-10). More details about this arrangement and the use of OES can be found in Es-sebbar et al. (2009).

In addition to both apparatuses described above, a Fourier transform infrared spectrometer (Bruker Equinox-55) is used to acquire the CO_2 (CO_2, 99.99% from Linde gas) actinometry measurements. In this case, the microwave discharge is connected to a multi-reflection white cell containing CO_2 gas. The infrared absorption cell has an optical path length (L) of 1040 cm and a volume (V) of $(3042 \pm 3)\ cm^3$. Before each series of experiments, the cell is pumped down to 10^{-5} mbar to prevent any contamination.

The spectral irradiance and the photon flux are determined by recording the temporal evolution of the CO (absorption band at 2143 cm^{-1}) resulting from the photodissociation of CO_2. The production of CO is recorded as a function of the irradiation time with a spectral resolution of 0.5 cm^{-1}. The variation of the CO density is determined by systematic comparison of synthetic and experimental spectra using the spectroscopic parameters from the GEISA database (Jacquinet-Husson et al. 2011). More details can be found in Romanzin et al. (2010) and Es-sebbar et al. (2015).

3. Results

3.1. Analysis of VUV Emission Spectra

VUV spectra from microwave plasmas in pure Ar, as well as in Ar/H_2 and H_2/He/Ar gas mixtures, are shown in Figures 2–4). VUV spectra in pure H_2 and He have already been described in Es-sebbar et al. (2015). To clarify, the spectra are either presented in logarithmic scale (i.e., Figure 2) or divided into two wavelength regions (Figures 3–4). It is worth noting that the emission intensities are not corrected by the spectral response of the grating and the sensitivity of the detector, since their wavelength dependence is negligible in the considered spectral range.

3.1.1. Pure Ar

The VUV emission spectrum obtained with pure Ar provided in Figure 2 is similar to those obtained for different kinds of plasma discharges (see, for example, Merbahi et al. 2004; Masoud et al. 2005). The most striking feature is the presence of a strong Lyα line (121.6 nm). Many other VUV features, including neutral excited species of nitrogen N I (119.9/149.4/174.5 nm), oxygen O I (130.5 nm), carbon monoxide CO I (156.3 nm), and carbon C I (165.7/193.5 nm) are also observed, arising from ubiquitous impurities as well as (O_2, N_2) traces of small air leaks and (H_2O, CO_2) remnants. The main source of those emissions is collisional energy transfers from Ar* metastables to N and O atoms (Wertheimer et al. 1999). They were also observed in many other plasma sources of pure Ar, like pulsed electric discharges (see Gedanken et al. 1972), and in high-pressure hollow cathode discharges (see Moselhy et al. 2003).

It should be emphasized that the $Ar_2{}^*$ excimer emission near 128 nm, due to radiative decay to the ground state of Ar atoms via the three-body reaction (i.e., $Ar^* + Ar + M \rightarrow Ar_2{}^* + M$), is not observed in our spectrum, unlike the work of Moselhy et al. (2003). This absence is probably due to the low pressure operations and also low electron densities of our plasma source, which does not have enough energy to produce resonant excited states. Thus, production of efficient excimer requires large densities of electrons with sufficient energy to excite the gas. As discussed by Schoenbach et al. (1997) and Moselhy et al. (2003), more intense excimer emissions from excited Ar* metastable were observed from plasmas that operated at high pressure with the presence of a large concentration of high-energy electrons, exceeding 15 eV. In this case, the number of three-body collisions becomes relevant due to high gas density and the collisional rates producing $Ar_2{}^*$. Under our experimental conditions, the maximum electron densities are of the order of $10^{12}\ cm^{-3}$ (Sá et al. 1991; Tatarova et al. 2005; Wijtvliet et al. 2009; Es-sebbar et al. 2010; Espinho et al. 2013), which is lower, by more than three orders of magnitude, than the hollow cathode discharge of Moselhy et al. (2003).

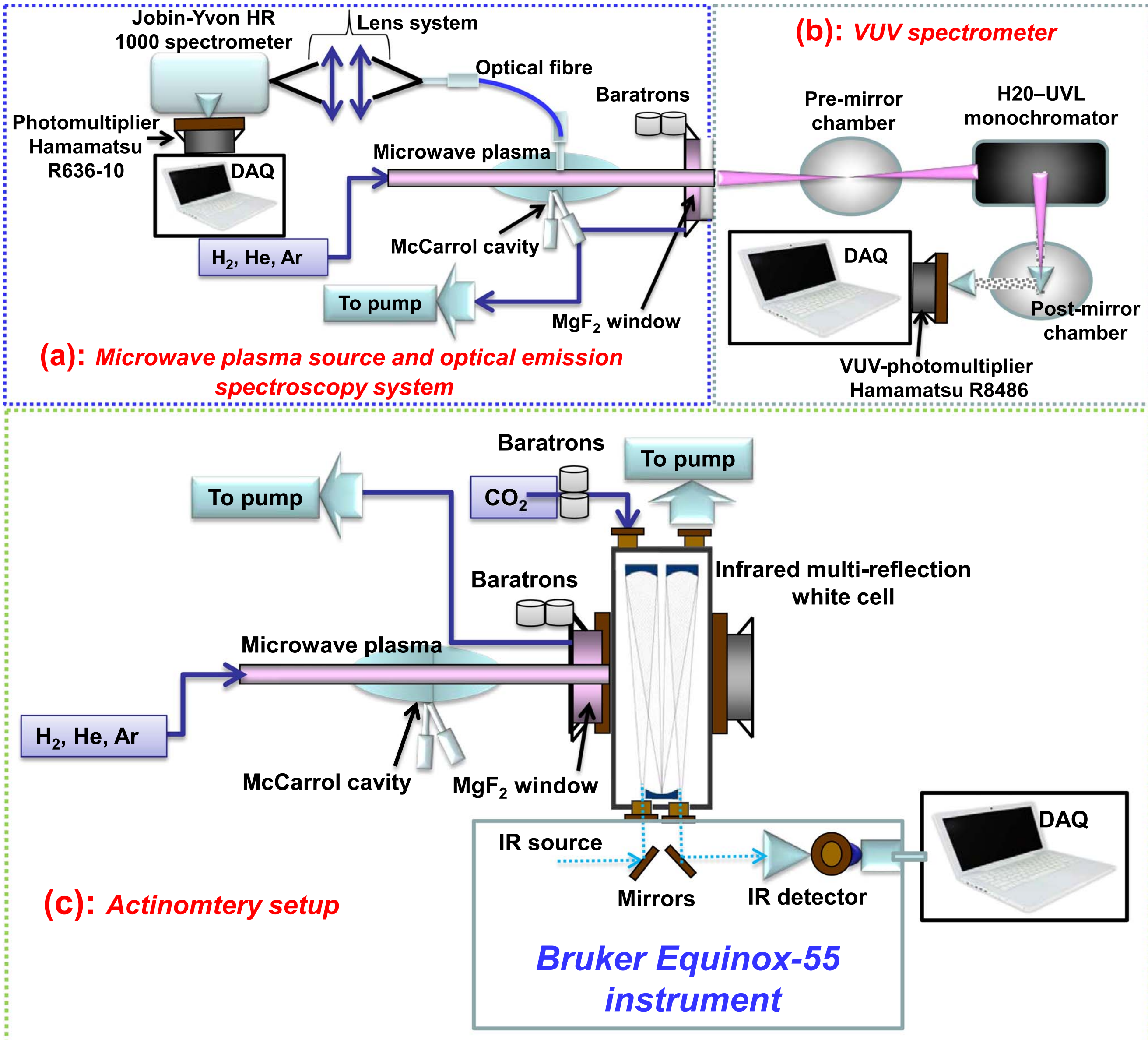

Figure 1. Experimental setup and diagnostics: (a) microwave plasma and optical emission spectroscopy; (b) VUV spectrometer; and (c) actinometry arrangement for spectral irradiance measurements.

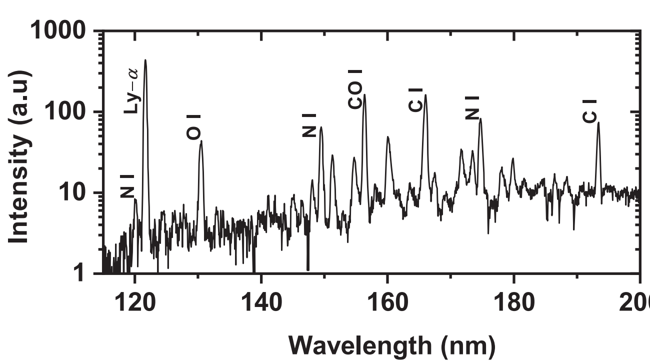

Figure 2. A typical VUV emission spectrum recorded from a microwave plasma sustained in pure Ar. Neutral excited species of nitrogen (N I), oxygen (O I), carbon (C I), and carbon monoxide (CO I), along with the Lyα line are identified in the spectrum. Operation conditions are as follows: a flow rate of 76.6 sccm, total gas pressure = 4.6 mbar, and a discharge power of 100 W.

Our conclusion for the VUV spectrum in pure argon is that small trace amounts of impurities, ($O_2 < 2$ ppm; $H_2O < 3$ ppm; $CH_4 < 0.5$ ppm), can evidently serve as precursors, yielding intense Lyα and other weak atomic emissions.

3.1.2. Ar/H_2 Mixture

Typical Ar/H_2 spectra are depicted in Figure 3, which mainly focuses on the emission features observed in the range 120.8–122.4 nm (Figure 3(a)) and 154–168 nm (Figure 3(b)) for different amounts of H_2 in Ar (i.e., 0%–2.12%). The spectra are strongly dominated by Lyα and some impurity lines such as CO I (156.3 nm) and C I (165.7 nm), but their intensities decrease with increasing H_2 concentration. Another important emission dominating the spectrum can be assigned to the $H_2(B^1_u–X^1_g)$ molecular band, with increasing intensity for higher percentages of H_2 in Ar. Other smaller impurity features of O I

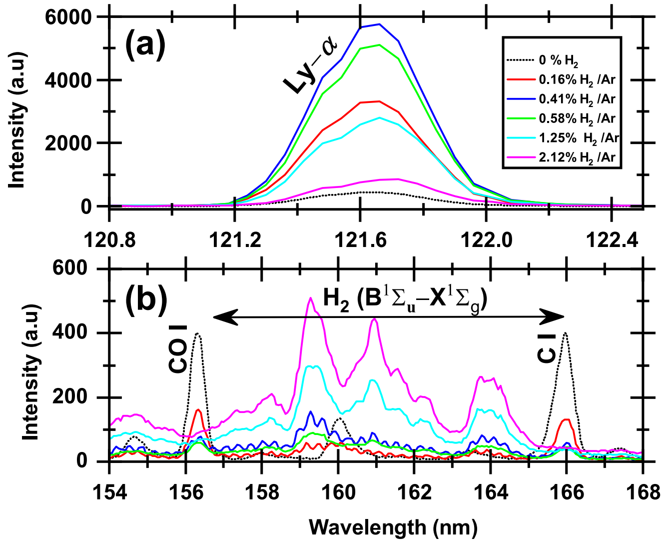

Figure 3. VUV emission spectra from microwave plasma generated in different H_2/Ar mixtures: 0.16%–2.12% H_2 in Ar. As a reference, the dotted lines present the spectrum obtained in pure Ar. The total gas pressure is 4.5 mbar, the flow rate is 15 sccm, and the microwave power is 100 W.

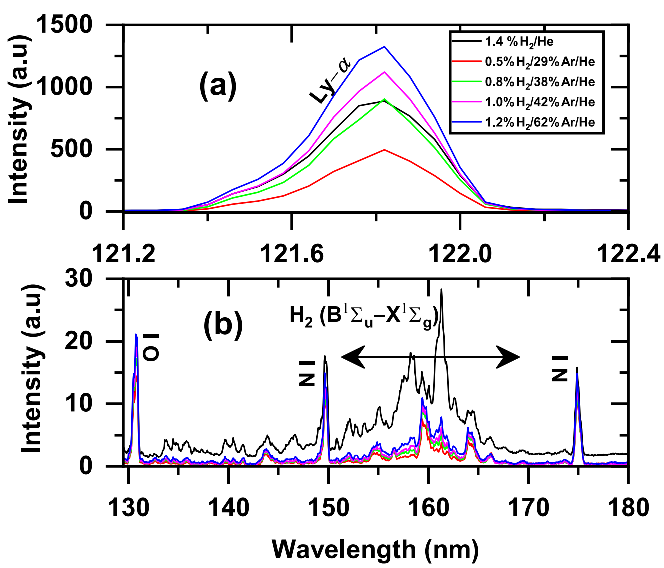

Figure 4. VUV emission spectra in $H_2/He/Ar$ plasma for (a) Lyα and (b) $H_2(B^1\Sigma_u$–$X^1\Sigma_g)$, along with some line impurities at a total pressure of 4.6 mbar, a discharge power of 100 W, and a flow rate of 15 sccm and for different compositions of the ternary mixture. The VUV spectrum in the binary mixture of 1.4% H_2/He is also shown.

(130.5 nm) and N I (149.5/174.5 nm) neutral excited species are also identified in the spectra.

We conclude that with the addition of small amounts of H_2 in Ar, the Lyα emission increases significantly, reaching a maximum for the 0.41% H_2/Ar mixture, while the H_2 $(B^1\Sigma_u$–$X^1\Sigma_g)$ band emissions remain very low. A further increase in H_2 concentrations leads to decreasing Lyα emission, while the $H_2(B^1\Sigma_u$–$X^1\Sigma_g)$ band emissions begin to increase. We emphasize in Figure 3 the absence of $H_2(B^1\Sigma_u$–$X^1\Sigma_g)$ band emissions in pure Ar microwave plasma.

The intense emission of Lyα for low H_2 concentrations (i.e., <0.41%) is attributed to excited hydrogen atoms due to the high electron density at low gas pressure; resulting in a more populated resonant H ($n = 2$) level that decays radiatively to the H ($n = 1$) ground state emitting the Lyα line. In addition to direct electron impact excitation, other processes involved in the population of the H ($n = 2$) excited state are charge transfer, with recombination between Ar^+ ions and H_2 leading to the formation of ArH^+ and H_2^+ molecular ions ($Ar^+ + H_2 \rightarrow ArH^+ + H$; $Ar^+ + H_2 \rightarrow H_2^+ + Ar$; see Thomas et al. 1997; Fozza et al. 1998). Thus, dissociation of the latter due to electron attachment processes yielded the excited H^* atoms ($ArH^+ + e^- \rightarrow Ar + H^*$; $H_2^+ + e^- \rightarrow H + H^*$) and subsequently Ly$\alpha$ line emissions (see Thomas et al. 1997; Fozza et al. 1998). Additionally, energy transfer related to the Ar ($^3P_2$) metastable with H_2 molecules should be considered and may play a role in producing the excited state of H atoms and then a further increase in Lyα emissions ($Ar(^3P_2) + H_2 \rightarrow Ar + H + H$; $Ar(^3P_2) + H_2 \rightarrow ArH^* + H$, $Ar(^3P_2) + H \rightarrow ArH^* \rightarrow Ar + H$ ($n = 2$); Fozza et al. 1998).

In contrast, as the percentage of H_2 increases, the electron density decreases and a depletion of the high-energy tail of the electron energy distribution function (eedf) occurs, which causes a drop in the electron excitation rates (Thomas et al. 1997; Fozza et al. 1998). In this case, processes responsible for the formation of H excited atoms and Lyα line emissions are reactions between charged particles of H^+, H_2^+, and H_3^+ or excited species with H_2 (Thomas et al. 1997; Fozza et al. 1998).

3.1.3. Ar/H$_2$/He Mixture

As revealed in our previous study by Es-sebbar et al. (2015), the optimized concentration of H_2 in He to achieve a maximum intensity of Lyα emissions is approximately 1%. In $H_2/Ar/He$, various mixtures have been tested for the ternary mixtures with the aim of studying the effect of gas compositions on Lyα and $H_2(B^1\Sigma_u$–$X^1\Sigma_g)$ emissions.

Figure 4 shows the spectra obtained with different mixtures at a total pressure of 4.6 mbar, a flow rate of 15 sccm, and a microwave power of 100 W. We observe that the addition of Ar modifies the emission intensities compared to those obtained for the binary mixture with 1.4% H_2/He, which is displayed for comparison. Compared to the binary mixture, the Lyα intensity increases by approximately a factor of 2 in the ternary mixture with 1.2% $H_2/62\%$ Ar/He, while the $(B^1\Sigma_u$–$X^1\Sigma_g)$ emission band decreases by about 60%. O I and N I trace emissions are also present in the ternary mixtures (Wertheimer et al. 1999). We emphasize a small increase in the intensity of O I but a decrease in the two line impurities of nitrogen in all gas mixtures containing Ar. Those results are very important for irradiation experiments, where a quasi-monochromatic Lyα line emission is needed to reproduce the solar irradiation. We also observe that increasing the Ar concentration, from 29% to 62% in H_2/He, does not diminish significantly the $(B^1\Sigma_u$–$X^1\Sigma_g)$ band intensity. Furthermore, the intensities of the impurity lines stay extremely low in all gas mixtures containing Ar. Their integrated intensities account for less than 8% of the total intensity between 115 and 180 nm.

The remarkable effects of the rare gases that were added to H_2 through VUV emissions and led to intense features, are in large part a consequence of the extremely efficient energy transfer from long-lived He* and Ar* metastables to H_2 and the trace amounts of impurities (Wertheimer et al. 1999). Those species contribute to an increase in the production of H excited states and subsequently in the Lyα feature. Table 1 lists metastable species together with the available energies that could be involved in the excitation processes of H_2 molecules.

Table 1
Excited Species of Ar and He, together with the Energy Reservoirs Involved in the Energy Transfer Processes of H_2

Excited Specie	Energy (eV)
Ar ($^3P_0$)	11.55
Ar ($^3P_2$)	11.72
He (2s $^3S_0$)	19.82
He (2s $^1S_0$)	20.61

Because only 4.48 and 10.2 eV of energies are required to respectively dissociate H_2 molecules and to excite the produced H atoms, Ar* and He* metastables represent an important energy reservoir, in addition to a direct electron excitation pathway (Fozza et al. 1998; Wertheimer et al. 1999; Masoud et al. 2005; Rahman et al. 2004). Moreover, they are also responsible for N I and O I line impurity emissions because the dissociation energies of N_2 and O_2 are only 9.85 and 5.08 eV, respectively.

3.2. Visible and IR Emission Spectra

Complementary experiments using OES in the visible and infrared ranges have been conducted with H_2/He and $H_2/He/Ar$ plasmas to observe the effect of Ar on the main emission features over a 300–900 nm spectral window. Results are shown in Figure 5 for only two gas mixtures, 1.4% H_2/He and 1.4% $H_2/27\%$ Ar/He. The spectra are dominated by neutral excited species of He I and H I emissions in the binary mixture and in the ternary mixture. However, the addition of Ar produces significant variation in the intensity. We observe that some He I emissions completely vanish in the presence of Ar (e.g., He I lines at 318.77, 381.96, 388.86, 438.79, 447.15, 501.57 nm). In contrast, the most apparent effect is that Ar I (e.g., metastables), along with H I emissions in the near-infrared, dominates the spectrum when Ar is included in the gas mixture.

3.3. Actinometry and Spectral Irradiance

In parallel with the abovementioned effort to characterize microwave plasma emissions using VUV-, visible-, and IR-optical emission spectra, the present work was also dedicated to investigating the effects that Ar addition in H_2/He has on the spectral irradiance and on the photon flux. As described in our previous work (Es-sebbar et al. 2015), chemical actinometry is based on the quantification of CO produced by the VUV photolysis of CO_2. Actinometry experiments were conducted for the six different cases listed in Table 2. A spectral simulation based on the GEISA database is used to derive the CO column density from the recorded infrared absorbance (see Figure 6); in this example, the microwave plasma is operated in the ternary gas mixture of 1.64% H_2 in (18% Ar/He) at a total pressure of 5.9 mbar. Due to the strong absorption coefficients of CO_2 in the VUV, the formation of CO due to CO_2 photolysis is very fast (a few minutes).

The absolute spectral irradiance (Φ_λ^{abs}) in units of ph s^{-1} cm^{-2} nm^{-1} is expressed as

$$\Phi_\lambda^{abs} = \frac{\Phi_\lambda^{rel}}{S}\frac{V}{L}\frac{dN(CO)}{dt}\frac{1}{\int \Phi_\lambda^{rel}\eta_\lambda\varepsilon_\lambda d\lambda}, \quad (1)$$

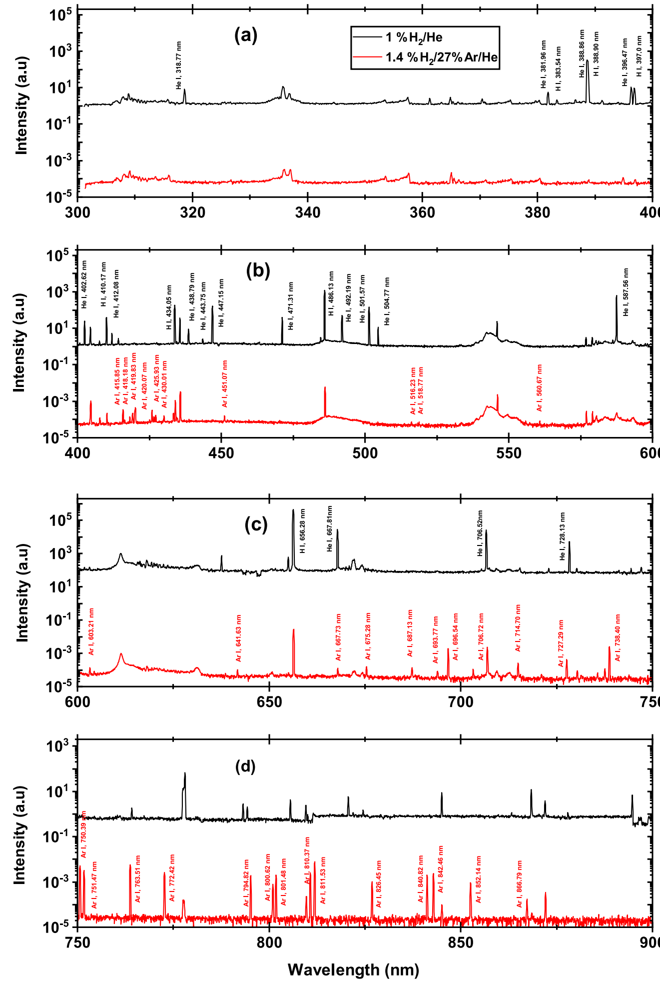

Figure 5. Optical emission spectra for gas mixtures of 1.4% H_2/He (black line) and 1.4% $H_2/27\%$ Ar/He (red line). The total pressures are 4.5 and 6.4 mbar, respectively. The microwave power is 100 W. For clarity, the spectra are given in logarithmic scale and slightly shifted.

where ϕ_λ^{rel} is the relative emission spectrum of the lamp (in unit of nm^{-1}) normalized to 1 (i.e., $\int \phi_\lambda^{rel} d\lambda = 1$), the quantity S is the area of the MgF_2 output window of the lamp ($S = 1\ cm^2$) and $dN(CO)/dt$ is the temporal variation of the CO column density during CO_2 photolysis (in units of molecules cm^{-2} s^{-1}). The two parameters V and L are respectively the volume of the infrared cell in which the CO_2 photolysis takes place and the optical path length, as defined in Section 2. The quantum yield (η_λ) of CO production from CO_2 photolysis is assumed to be equal to unity and the fraction (ε_λ) of the photon flux absorbed by CO_2 is given by

$$\varepsilon_\lambda = 1 - \exp(-\sigma_\lambda\, l\, p), \quad (2)$$

where σ_λ is the CO_2 absorption cross section (in units of atm^{-1} cm^{-1}) (Yoshino et al. 1996; Venot et al. 2013), $l = 22$ cm is the transverse length of the absorption cell, and p is the partial pressure of CO_2 (in atm units). As detailed previously (Es-sebbar et al. 2015), the irradiance of the light source is calculated using the "polychromatic" method, $I_{\lambda 1-\lambda 2}^{poly}$ (in units of ph cm^{-2} s^{-1}), taking into account the entire spectrum of the lamp. The irradiance of the light source from

Table 2
Actinometry Experiments Using Photolysis of CO_2 in N_2 by Microwave Discharge Generated for Various Gas Mixture Rules

Actinometry Case	Microwave Plasma Mixture Rule	Operated Pressure of the Plasma (mbar)	$dN(\mathrm{CO})/dt$ (10^{13} molecules $\mathrm{cm}^{-2}\ \mathrm{s}^{-1}$)
Act 1	1.4% H_2/He	4.8	4.26
Act 2	1.01% H_2/49% Ar/He	9.4	6.24
Act 3	1.28% H_2/35% Ar/He	7.4	9.44
Act 4	1.41% H_2/29% Ar/He	6.8	9.13
Act 5	1.56% H_2/22% Ar/He	6.1	7.81
Act 6	1.64% H_2/18% Ar/He	5.9	8.16

Note. The microwave power is constant and settled at 100 W. The slope $dN(\mathrm{CO})/dt$ is measured to determine the photon flux at Lyα. In all experiments, the pressure of CO_2 is 5.3 and 661 mbar of N_2 is added in the cell to avoid absorption saturation effects.

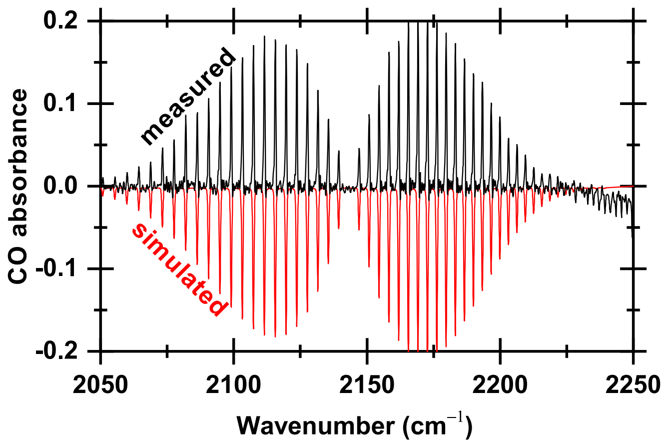

Figure 6. Comparison of measured and calculated absorbances of CO; the spectral resolution is 0.5 cm^{-1}. Actinometry was performed at 0.8% CO_2/N_2 with a total pressure of 661 mbar, and the photolysis time was 1800 s.

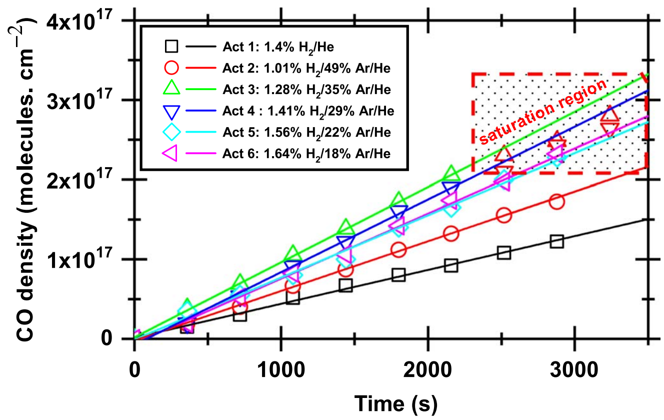

Figure 7. Evolution of the CO column density from CO_2 photolysis by microwave discharge using the various gas mixtures listed in Table 2. In all cases, the CO_2 gas pressure is 5.3 mbar in 661 mbar of N_2. Linear fits have been used to determine the dN (CO)/dt slope.

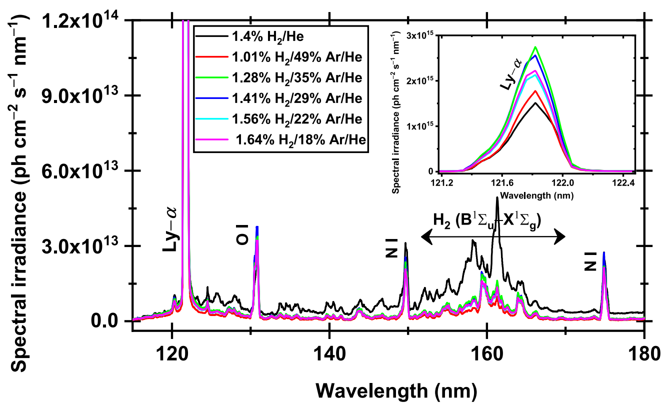

Figure 8. Measured spectral irradiances for all six cases described in Table 2.

this method is then calculated through the integration of the spectral irradiance following

$$I^{\mathrm{poly}}_{\lambda1-\lambda2} = \int_{\lambda1}^{\lambda2} \Phi^{\mathrm{abs}}_{\lambda} d\lambda. \tag{3}$$

The CO column densities show a linear dependence with irradiation time (Figure 7). A linear fit yields the slope dN (CO)/dt. To increase the accuracy, a series of eight to nine spectra were recorded every 6 minutes and then averaged. High correlation coefficients were obtained for each linear fit. It should be emphasized that for the 1.28% H_2/35% Ar/He and 1.41% H_2/29% Ar/He mixtures, saturation appeared for CO column densities larger than 2.2×10^{17} molecule cm^{-2} (i.e., $\geqslant$2520 s) due to the high photon flux delivered by the microwave plasma.

Figure 8 shows the spectral irradiances measured for five ternary mixtures and one binary mixture (microwave power = 100 W). We observe that the photon flux at Lyα is larger with the presence of Ar and that a maximum value of 2.70×10^{15} ph $\mathrm{cm}^{-2}\ \mathrm{s}^{-1}\ \mathrm{nm}^{-1}$ is reached for the 1.28% H_2/35% Ar/He gas composition. It is greater by a factor of 1.8 compared to the value obtained for the binary mixture 1.4% H_2/He. Note that for the gas mixture where the maximum absolute photons flux is reached, we also have an optimum for the monochromaticity because emission in the $H_2(B^1\Sigma_u–X^1\Sigma_g)$ region does not vary significantly. This gas mixture is therefore recommended to best mimic the solar spectrum.

Since the emission spectrum is principally dominated by Lyα and $H_2(B^1\Sigma_u–X^1\Sigma_g)$, a quantitative comparison of the integrated spectral irradiances was performed. Lyα irradiance was integrated between 120 and 124 nm and the $H_2(B^1\Sigma_u–X^1\Sigma_g)$ band between 150 and 170 nm. The results shown in Table 3 were obtained with a rigorous calculation that takes into account the entire spectrum of the lamp. In the binary mixture, the ratio of the Lyα to the $H_2(B^1\Sigma_u–X^1\Sigma_g)$ band is approximately 2. In the presence of Ar, this ratio increases by a factor of 4.3.

Accounting for the monochromatic method, it is evident that the integrated photon flux is relatively higher compared to the polychromatic flux at Lyα (see Es-sebbar et al. 2015). Based on our previous studies (Bénilan et al. 2011), Orlando et al. (Dawley et al. 2014; Shi et al. 2015) were the first to use microwave plasmas in the ternary mixture of 2% H_2/18% Ar/He mixture for irradiation experiments to mimic reactions that may occur in

Table 3
Integrated Spectral Irradiances for Various Wavelength Intervals

Actinometry Case	$I^{poly}_{120-124\ nm}$ (10^{14} ph cm^{-2} s^{-1})	$I^{poly}_{150-170\ nm}$ (10^{14} ph cm^{-2} s^{-1})	$I^{poly}_{120-180\ nm}$ (10^{14} ph cm^{-2} s^{-1})	$\frac{I^{poly}_{120-124\ nm}}{I^{poly}_{120-180\ nm}}$ (%)	$\frac{I^{poly}_{120-124\ nm}}{I^{poly}_{150-170\ nm}}$
1.4% H_2/He	5.47	2.76	10.43	52.4	1.98
1.01% H_2/49% Ar/He	5.85	0.686	7.33	79.8	8.5
1.28% H_2/35% Ar/He	8.94	1.050	11.16	80.1	8.5
1.41% H_2/29% Ar/He	8.76	1.020	10.85	80.7	8.6
1.56% H_2/22% Ar/He	7.37	0.867	9.20	80.1	8.5
1.64% H_2/18% Ar/He	7.70	0.907	9.61	80.1	8.5

interstellar regions and Titan's upper atmospheres. They measured a Lyα photon flux of (2.7–4) $\times$ 10^{14} cm^{-2} s^{-1} for a microwave plasma operated at gas pressure of ~4.7 mbar, a flow rate of 15 sccm, and lower discharge powers ~20–50 W. Their corresponding data remain lower by approximately one order of magnitude compared to our calculated value in the considered mixture of 1.64% H_2/18% Ar/He at 100 W. Our higher flux might be simply related to a higher power operation.

A full description of the specific gas-kinetic process and energy transfer in Ar/H_2/He would be required to explain the dependence of VUV irradiances on gas mixtures. Moreover, because the current emphasis in experimental studies is on only measuring VUV emissions and spectral irradiances , a full understanding of the mechanisms affecting the VUV emissions in the ternary mixture is beyond the scope of this paper. Nevertheless, in addition to the mechanisms mentioned in Section 3.1, a changing gas composition is expected to strongly affect fundamental parameters such as gas density, temperature, and the electron energy distribution function of electrons, which in turn affects VUV emission (Thomas et al. 1997; Fozza et al. 1998; Mills & Ray 2002; Mills et al. 2002; Rahman et al. 2004). Thus, additional measurements such as the densities of extremely efficient Ar* and He* metastables, electron densities, and detailed kinetic modeling, are required to gain more insight into the possible channels governing VUV emission in ternary gas mixtures.

3.4. Comparison with Solar Data

A quantitative comparison between VUV spectral irradiances obtained with microwave discharge and solar data is important because the goal is to compare the energy deposition. We present in Figure 9 a comparison between the solar spectra taken from "Atlas 3" (Thuillier et al. 2004) and our optimized VUV spectra obtained with the 1.28% H_2/35% Ar/He mixture. The spectral irradiances of the binary mixture with 1.4% H_2/He and also 1% H_2/He obtained in our previous study (Es-sebbar et al. 2015) are also shown. The Atlas 3 composite spectrum used as a reference for comparison exhibits a resolution of 0.25 nm. This spectral resolution is the highest among the absolute reference solar spectral irradiance (SSI); even considering the recent valuable efforts of Haberreiter et al. (2017) to create a time-dependent composite SSI, within a resolution of 1 nm. It should be noted that the ATLAS 3 spectrum illustrated in Figure 9 is associated with low solar activity levels. Nevertheless, even for high levels of solar activity we do not expect the relative comparison to be significantly different. Even if the VUV part of the SSI varies as much as 50% during the solar cycle, the relative

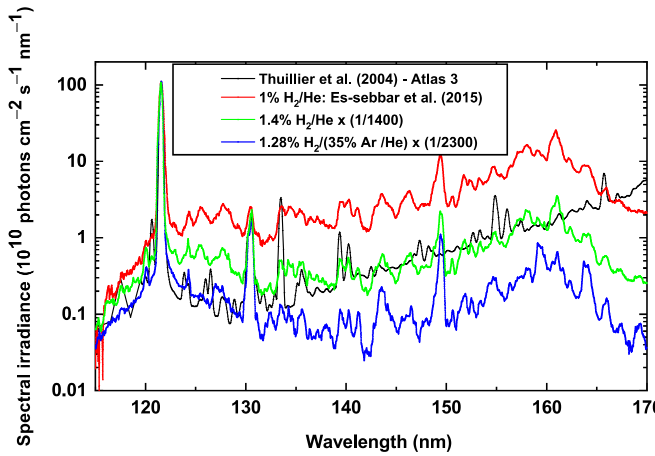

Figure 9. Quantitative comparison between our measured spectral irradiances and data taken from "Atlas 3"; (Thuillier et al. 2004). Our previous measurements for 1% H_2/He are also shown (Es-sebbar et al. 2015). The spectrum with 1.4% H_2/He (green line) has been divided by 1400 to scale the Lyα emission line to the solar one, while the measured spectrum in 1.28% H_2/35% Ar/He has been divided by 2300 to scale both the Lyα line and the $H_2(B^1\Sigma_u$–$X^1\Sigma_g)$ band to the solar data of Atlas-3.

spectral irradiance between the Lyα line (121.6 nm) and 170 nm is expected to show variations of less than about 10% during a typical solar cycle (Haberreiter et al. 2017).

Our results reveal that the ternary mixture yielded quasi-monochromatic light emission that is dominated by a Lyα line contribution with low $H_2(B^1\Sigma_u$–$X^1\Sigma_g)$ band emission, and minimum emission of impurity features. Consequently, we conclude that the emission with a ternary mixture can be advantageously used as a quasi-monochromatic source to simulate the solar energy deposition at Lyα only. In our experimental conditions, the spectral irradiance from the microwave discharge is higher by a factor of close to 2300 compared to the measured solar irradiance at Earth, which can help us study long-timescale photochemical processes. Compared to 1% H_2/He, the irradiance from the binary mixture with 1.4% H_2/He over the range 115–170 nm, best reproduces the solar spectra, and resembles quite accurately both Lyα and $H_2(B^1\Sigma_u$–$X^1\Sigma_g)$ shapes when it is scaled by a factor of 1400. Therefore, it can be suited to use this binary mixture to obtain the best simulator of the entire VUV solar spectrum in the 115–170 nm range. Obviously, the difference in the retrieved scaling factor of the measured spectral irradiances used for quantitative comparison with solar data is fully related to the relevant operating experimental parameters of the microwave plasma, which include the initial mixture composition, gas pressure, flow rates, and also input power.

Clearly, the current bulk of spectral irradiance data from this study emphasizes the importance of controlling the specific spectral window of 115–170 nm and could be crucial for irradiation ice analogs and derivation of photodesorption yields for astrophysical interests. For example, in recent years, there have been attempts to systematically report a variation in CO photodesorption yields up to two orders of magnitudes (see Öberg et al. 2007, 2009; Muñoz Caro et al. 2010; Chen et al. 2014; Ligterink et al. 2015; Paardekooper et al. 2016). Notwithstanding recent experimental developments using synchrotron facilities to investigate the photon energy dependence for ice analog irradiations and derivation of photodesorption rates (Fayolle et al. 2011; Bertin et al. 2012; Fayolle et al. 2013), most experimental studies using microwave plasmas provide photodesorption rates for photons at either a specific energy (essentially Lyα) or for very broad VUV wavelength ranges. Such variations in the photon sources used for irradiation, without a complete characterization of the source, could explain the observed discrepancies in CO photodesorption yields.

4. Conclusion

We have studied the effects of Ar added to H_2/He microwave plasmas on the VUV and visible emission by combining various diagnostics that include VUV and OES. The main goal was to determine spectral irradiances in various ternary gas mixtures. Results show that the addition of Ar into H_2/He mixtures largely affects both Lyα line and $H_2(B^1\Sigma_u–X^1\Sigma_g)$ band emissions. The spectral irradiance at Lyα is larger with the presence of Ar, with a maximum of 2.70×10^{15} ph cm^{-2} s^{-1} nm^{-1} obtained for the 1.28% H_2/35% Ar/He mixture; this is larger by a factor of 1.8 compared to the value in the binary mixture. Additionally, the appropriate ternary mixture of 1.28% H_2/35% Ar/He plasma leads to a quasi-monochromatic spectrum that is dominated by the Lyα line. The measured spectral irradiance in the range 115–170 nm is almost 4 orders of magnitude higher than the solar irradiance at Earth, which could help us study long-timescale photochemical processes in laboratory astrophysical simulations.

We gratefully acknowledge the French Space Agency (Centre National d'Etudes Spatiales, CNES), the Ile de France Region (SESAME grant), and the French National Program of Planetary Sciences (PNP) for their financial support of the SETUP program. The authors gratefully acknowledge the CNES and the IPSL for their financial support in the frame of the EXPOSE International Space Station Program. Et. Es. thanks Université Paris-Est Créteil (UPEC) for providing financial support.

ORCID iDs

Et-touhami Es-sebbar https://orcid.org/0000-0002-4099-2599
Hervé Cottin https://orcid.org/0000-0001-9170-5265

References

Baratta, G. A., Leto, G., & Palumbo, M. E. 2002, A&A, 384, 343
Bénilan, Y., Gazeau, M.-C., Es-sebbar, Et., et al. 2011, in EPSC-DPS Joint Meeting, Nantes, France 6, 1317
Bergonzo, P., Patel, P., Boyd, I. W., & Kogelschatz, U. 1992, ASSc, 54, 424
Bertin, M., Fayolle, E. C., Romanzin, C., et al. 2012, PCCP, 14, 9929
Chen, Y.-J., Chuang, K. J., Muñoz Caro, G. M., et al. 2014, ApJ, 781, 15
Cottin, H., Moore, M. H., & Bénilan, Y. 2003, ApJ, 590, 874
Cruz-Diaz, G. A., Muñoz Caro, G. M., Chen, Y.-J., & Yih, T.-S. 2014, A&A, 562, A119
Davis, D., & Braun, W. 1968, ApOpt, 7/10, 2071
Dawley, M. M., Pirim, C., & Orlando, T. M. 2014, JPCA, 118, 1228
El-Dakrouri, A., Yan, J., Gupta, M. C., Laroussi, M., & Badr, Y. 2002, JPhD, 35, L109
Espinho, S., Felizardo, E., Tatarova, E., Dias, F.-M., & Ferreira, C. M. 2013, JAP, 102, 114101
Es-sebbar, Et., Benilan, Y., Fray, N., et al. 2015, APJS, 218, 19
Es-sebbar, Et., Benilan, Y., Jolly, A., & Gazeau, M.-C. 2009, JPhD, 42, 135206
Es-sebbar, Et., Gazeau, M.-C., Benilan, Y., Jolly, A., & Pintassilgo, C. D. 2010, JPhD, 43, 335203
Fayolle, E. C., Bertin, M., Romanzin, C., et al. 2011, ApJL, 739, L36
Fayolle, E. C., Bertin, M., Romanzin, C., et al. 2013, A&A, 556, A122
Fozza, A. C., Kruse, A., Hollander, A., Ricard, A., & Wertheimer, M. R. 1998, JVST, 16, 72
Gedanken, A., Szoke, A., Raz, B., & Jortner, J. 1972, JChPh, 57, 3456
Haberreiter, M., Schöll, M., Dudok de Wit, T., et al. 2017, JGRA, 122, 5910
Hollander, A., & Wertheimer, M. R. 1994, JVST, 12, 879
Jacquinet-Husson, N., Crepeau, L., Armante, R., et al. 2011, JQSRT, 112, 2395
Ligterink, N. F. W., Paardekooper, D. M., Chuang, K. J., et al. 2015, A&A, 584, A56
Masoud, N., Martus, K., & Becker, K. 2005, JPhD, 38, 1674
McCarthy, T. J., Murnick, D. E., Salvermoser, M., & Ulrich, A. 2005, JPhB, 38, 3043
Merbahi, N., Sewraj, N., Marchal, F., Salamero, Y., & Millet, P. 2004, JPhD, 37, 1664
Mills, R. L., & Ray, P. 2002, NJPh, 4, 22
Mills, R. L., Ray, P. C., Dhandapani, B., Mayo, R. M., & He, J. 2002, JAPh, 92, 7008
Moselhy, M., Petzenhauser, I., Frank, K., & Schoenbach, K. H. 2003, JPhD, 36, 2922
Muñoz Caro, G. M., Jiménez-Escobar, A., Martín-Gago, J. Á, et al. 2010, A&A, 522, A108
Öberg, K. I., Fuchs, G. W., Awad, Z., et al. 2007, ApJL, 662, L23
Öberg, K. I., van Dishoeck, E. F., & Linnartz, H. 2009, A&A, 496, 281
Paardekooper, D. M., Fedoseev, G., Riedo, A., & Linnartz, H. 2016, A&A, 596, A72
Rahman, A., Yalin, A. P., Surla, V., et al. 2004, PSST, 13, 537
Rajappan, M., Buttner, M., Cox, C., & Yates, J. T., Jr. 2010, JPCA, 114, 3443
Romanzin, C., Arzoumanian, E., Es-sebbar, Et., et al. 2010, P&SS, 58, 1748
Sá, A. B., Ferreira, C. M., Pasquiers, S., et al. 1991, JAP, 70, 4147
Schoenbach, K. H., El-Habachi, A., Shi, W. H., & Ciocca, M. 1997, PSST, 6, 468
Shi, J., Grieves, G. A., & Orlando, T. M. 2015, ApJ, 804, 24
Tatarova, E., Dias, F. M., Gordiets, B., & Ferreira, C. M. 2005, PSST, 14, 19
Thomas, L., Jauberteau, J. L., Jauberteau, I., et al. 1997, PChPPr, 17, 193
Thuillier, G., Floyd, L., Woods, T. N., et al. 2004, AdSpR, 34, 256
Venot, O. N., Fray, Y., Benilan, M.-C., et al. 2013, A&A, 551, A131
Wertheimer, M. R., Fozza, A. C., & Hollander, A. 1999, NIMPB, 151, 65
Wijtvliet, R., Felizardo, E., Tatarova, E., et al. 2009, JAP, 106, 103301
Yan, J. X., El-Dakrouri, A., Laroussi, M., & Gupta, M. C. 2002, JVST, 20, 2574
Yoshino, K., Esmond, J. R., Sun, Y., et al. 1996, JQRST, 55, 53